

Catalytic Activity of a Series of Zn(II) Phenoxides for the Copolymerization of Epoxides and Carbon Dioxide

Donald J. Darensbourg,* Matthew W. Holtcamp, Ginette E. Struck, Marc S. Zimmer, Sharon A. Niezgoda, Patrick Rainey, Jeffrey B. Robertson, Jennifer D. Draper, and Joseph H. Reibenspies

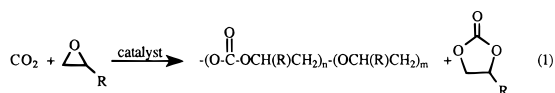
Contribution from the Department of Chemistry, Texas A&M University, P.O. Box 30012, College Station, Texas 77842

Received July 24, 1998

Abstract: A series of zinc phenoxides of the general formula $(2,6\text{-R}_2\text{C}_6\text{H}_3\text{O})_2\text{Zn}(\text{base})_2$ [R = Ph, ^tBu, ⁱPr, base = Et₂O, THF, or propylene carbonate] and $(2,4,6\text{-Me}_3\text{C}_6\text{H}_2\text{O})_2\text{Zn}(\text{pyridine})_2$ have been synthesized and characterized in the solid state by X-ray crystallography. All complexes crystallized as four-coordinate monomers with highly distorted tetrahedral geometry about the zinc center. The angles between the two sterically encumbering phenoxide ligands were found to be significantly more obtuse than the corresponding angles between the two smaller neutral base ligands, having average values of 140° and 95°, respectively. In a noninteracting solvent such as benzene or methylene chloride at ambient temperature, the ancillary base ligands are extensively dissociated from the zinc center, with the degree of dissociation being dependent on the base as well as the substituents on the phenolate ligands. That is, stronger ligand binding was found in zinc centers containing electron-donating *tert*-butyl substituents as opposed to electron-withdrawing phenyl substituents. In all instances, the order of ligand binding was pyridine > THF > epoxides. These bis(phenoxide) derivatives of zinc were shown to be very effective catalysts for the copolymerization of cyclohexene oxide and CO₂ in the absence of strongly coordinating solvents, to afford high-molecular-weight polycarbonate (*M*_w ranging from 45 × 10³ to 173 × 10³ Da) with low levels of polyether linkages. However, under similar conditions, these zinc complexes only coupled propylene oxide and CO₂ to produce cyclic propylene carbonate. Nevertheless, these bis(phenoxide) derivatives of zinc were competent at terpolymerization of cyclohexene oxide/propylene oxide/CO₂ with little cyclic propylene carbonate formation at low propylene oxide loadings. While CO₂ showed no reactivity with the sterically encumbered zinc bis(phenoxides), e.g., $(2,6\text{-di-}t\text{-butylphenoxide})_2\text{Zn}(\text{pyridine})_2$, it rapidly inserted into one of the Zn–O bonds of the less crowded $(2,4,6\text{-trimethylphenoxide})_2\text{Zn}(\text{pyridine})_2$ to provide the corresponding aryl carbonate zinc derivative. At the same time, both sterically hindered and sterically unhindered phenoxide derivatives of zinc served to ring-open epoxide, i.e., were effective catalysts for the homopolymerization of epoxide to polyethers. The relevance of these reactivity patterns to the initiation step of the copolymerization process involving these monomeric zinc complexes is discussed.

Introduction

The synthesis of select polycarbonates and/or cyclic carbonates via metal-catalyzed coupling reactions of carbon dioxide and epoxides (eq 1) has been extensively investigated as a potential pathway for the effective utilization of carbon dioxide.



Inoue and co-workers first reported on this process in 1969, employing a catalyst derived from Zn(CH₂CH₃)₂ and H₂O.^{1,2} During the intervening years, a variety of related catalysts and catalyst precursors containing zinc have been shown to promote this copolymerization process.³ The most active of these catalysts are those prepared by the reaction of zinc hydroxide or zinc oxide with dicarboxylic acids.⁴ Indeed, there is a commercial process based on these insoluble zinc catalysts;

* To whom correspondence should be addressed. E-mail: DJDARENS@mail.chem.tamu.edu.

(1) Inoue, S.; Koinuma, H.; Tsuruta, T. *J. Polym. Sci., Part B* 1969, 7, 287.

however, this method is plagued by low catalytic activity, thus requiring removal of the metal from the synthesized polymer by an acid wash.⁵ Other catalyst systems composed of double

(2) A brief review covering this and related work has appeared: Inoue, S. *Carbon Dioxide as a Source of Carbon*; Aresta, M., Forti, G., Eds.; Reidel Publishing Co.: Dordrecht, 1987; p 331. See also an earlier, more comprehensive review: Rokicki, A.; Kuran, W. *J. Macromol. Sci., Rev. Macromol. Chem.* 1981, C21, 135. An excellent current assessment of the status of catalysts for copolymerization processes utilizing CO₂ as a monomer has been published: Super, M. S.; Beckman, E. J. *Trends Polym. Sci.* 1997, 5, 236.

(3) (a) Inoue, S.; Koinuma, H.; Tsuruta, T. *Makromol. Chem.* 1969, 130, 210. (b) Inoue, S.; Koinuma, H.; Yokoo, Y.; Tsuruta, T. *Makromol. Chem.* 1971, 143, 97. (c) Kobayashi, M.; Inoue, S.; Tsuruta, T. *Macromolecules* 1971, 4, 658. (d) Kobayashi, M.; Tang, Y. L.; Tsuruta, T.; Inoue, S. *Makromol. Chem.* 1973, 169, 69. (e) Kobayashi, M.; Inoue, S.; Tsuruta, T. *J. Polym. Sci., Polym. Chem. Ed.* 1973, 11, 2383. (f) Kuran, W.; Pasykiewicz, S.; Skupinska, J.; Rokicki, A. *Makromol. Chem.* 1976, 177, 11. (g) Kuran, W.; Pasykiewicz, S.; Skupinska, J. *Makromol. Chem.* 1976, 177, 1283. (h) Soga, K.; Uenishi, K.; Hosada, H.; Ikeda, S. *Makromol. Chem.* 1977, 178, 893. (i) Soga, K.; Hyakkoku, K.; Ikeda, S. *Makromol. Chem.* 1978, 179, 2837.

(4) Soga, K.; Imai, E.; Hattori, I. *Polym. J.* 1981, 13, 407.

(5) (a) Rokicki, A. (Air Products and Chemicals, Inc., and Arco Chemical Co.). U.S. Patent 4,943,677, 1990. (b) Motika, S. (Air Products and Chemicals, Inc., Arco Chemical Co., and Mitsui Petrochemical Industries Ltd.). U.S. Patent 5,026,676, 1991.

metal cyanide complexes employed in this copolymerization process have obvious alternative environmental shortcomings.⁶

Recently, soluble zinc complexes have been discovered which possess significant catalytic activity to be attractive as catalysts for the production of high-molecular-weight polycarbonates from CO₂ and epoxides. One of these systems represents a modification of a process described in the patent literature which involves catalysts produced from the reaction of zinc oxide with acid anhydrides in alcoholic solvents or with the monoester of a dicarboxylic acid.⁷ This methodology has been notably improved upon by carrying out the esterification reaction in a long-chain perfluorinated alcohol (tridecafluorooctanol) to impart catalyst solubility in liquid or supercritical carbon dioxide.⁸ Although the explicit structure of this latter catalyst is unknown due to the unavailability of crystals suitable for crystallographic analysis, it was shown to be very active for the copolymerization of 1,2-epoxycyclohexane (cyclohexene oxide) and carbon dioxide.

In another major development in this area, we have communicated our results on the copolymerization of cyclohexene oxide/CO₂ and the terpolymerization of cyclohexene oxide/propylene oxide/CO₂ catalyzed by soluble, well-defined monomeric zinc complexes.⁹ These complexes consist of distorted tetrahedral zinc phenoxide derivatives which possess bulky substituents in the 2 and 6 positions of the phenolate ligands, with the coordination sphere of zinc being completed with two labile donor ligands. For example, (2,6-diphenylphenoxide)₂Zn^{II}(THF)₂ is a typical representative of this group of catalysts. Herein, we wish to describe the synthesis and characterization of a series of these zinc(II) complexes along with the catalytic activity of the aforementioned zinc derivatives for the copolymerization and terpolymerization of carbon dioxide and epoxides.

Experimental Section

Methods and Materials. All manipulations were carried out under an inert atmosphere unless otherwise stated, using glassware which was flame-dried prior to use. The solvents were freshly distilled before use. Cyclohexene oxide was purchased from Aldrich Chemical Co., and propylene oxide was purchased from Fluka Chemical Co., both were distilled over calcium hydride before use. 2,6-Diphenylphenol, 2,4,6-tri-*tert*-butylphenol, 2,6-di-*tert*-butylphenol, 2,4,6-tri-methylphenol, 2,6-di-isopropylphenol, and sodium bis-trimethylsilyl amide were purchased from Aldrich Chemical Co. ZnCl₂ dihydrate was purchased from Fischer and was dehydrated by the published procedure.¹⁰ Zn^{II}-(2,4,6-tri-*tert*-butylphenoxide)₂(THF)₂ was prepared according to the published procedure.¹¹ Infrared spectra were recorded on a Mattson 6021 spectrometer with DTGS and MCT detectors. ¹H and ¹³C NMR spectra were recorded on a Varian XL-200 or Unity+ 300 superconducting high-resolution spectrometer. Elemental analyses were carried out by Galbraith Laboratories Inc. and Canadian Microanalytical Services, Ltd.

Synthesis of (2,6-Diphenylphenoxide)₂Zn(diethyl ether)₂, 1. Complex **1** was prepared in a manner similar to that employed in the synthesis of (2,4,6-tri-*tert*-butylphenoxide)₂Zn(THF)₂, with only minor

differences.¹¹ A 1.0-g (7.3 mmol) amount of ZnCl₂ was combined with a 2.67-g (14.4 mmol) amount of sodium bis-trimethylsilyl amide in a 50-mL Schlenk flask equipped with a reflux condenser. After the addition of 30 mL of diethyl ether via syringe, the slurry was refluxed for 1 h; subsequent removal of the formed sodium chloride by filtration resulted in a colorless to pale yellow solution. A 3.61-g (14.7 mmol) quantity of 2,6-diphenylphenol dissolved in 15 mL of diethyl ether was added to the Zn^{II}(bis-trimethylsilyl amide)₂ solution via cannula. The solution was then concentrated under vacuum to less than one-half its original volume and placed in a freezer overnight. From this, 4.20 g of product (80.8% yield) was isolated as colorless crystals. ¹H NMR (CD₂-Cl₂): δ 1.13 (t, 12H); 3.28 (q, 8H); 6.65–7.65 (m, 2,6-Ph₂PhO-, 26H). Free diethyl ether and bound diethyl ether are in equilibrium in solution, with diethyl ether being predominantly free in deuterated dichloromethane. Anal. Calcd for C₄₄H₄₆O₄Zn: C, 75.04; H, 6.58. Found: C, 80.79; H, 5.60. In part, the inability to obtain a close match in elemental analyses is due to the ease with which the coordinated ether ligands are lost.

(2,6-Diphenylphenoxide)₂Zn(THF)₂, 2. This complex was prepared in a manner analogous to that described above for complex **1** by simply replacing diethyl ether with tetrahydrofuran as solvent for 2,6-diphenylphenol. A 4.00-g amount (77.8% yield) of product was isolated as colorless crystals. ¹H NMR (CD₂Cl₂): δ 1.72 (m, THF, 8H); 3.46 (m, THF, 8H); 6.65–7.65 (m, 2,6-Ph₂PhO-, 26H). Free THF and bound THF are in equilibrium in solution, and THF appears to be predominantly free in deuterated dichloromethane. Anal. Calcd for C₄₄H₄₂O₄Zn: C, 75.48; H, 6.05. Found: C, 73.91; H, 4.89.

(2,6-Diisopropylphenoxide)₂Zn(THF)₂, 3. This complex was prepared in a manner analogous to that described above using 0.5 g (3.7 mmol) of ZnCl₂, 1.4 g (7.6 mmol) of NaN(Si(CH₃)₃)₂, and 1.3 g of 2,6-diisopropylphenol. A 1.4-g (7.8 mmol) amount (67.6% yield) of product was isolated as colorless crystals. ¹H NMR (CD₂Cl₂): δ 1.15 (broad, 12H); 1.78 (m, 8H); 3.15 (broad, 4H); 3.65 (m, 8H); 6.65–7.2 (broad, PhO-, 6H). Anal. Calcd for C₃₂H₅₀O₄Zn: C, 68.13; H, 8.93. Found: C, 66.88; H, 8.14.

(2,6-Di-*tert*-butylphenoxide)₂Zn(THF)₂, 4. A 1-mL THF solution of 2,6-di-*tert*-butylphenol (0.214 g, 1.04 mmol) was added to a 1-mL THF solution of Zn[N(SiMe₃)₂]₂ (0.20 g, 0.52 mmol), leading to a colorless solution which was stirred at room temperature for 1 h. Approximately 2 mL of hexanes was added, and the clear solution was then placed at –20 °C. Colorless block crystals formed after several days. The supernate was removed, and the crystals were dried under vacuum and collected to yield 0.156 g (49%). Anal. Calcd for C₃₆H₅₈O₄Zn: C, 69.71; H, 9.43. Found: C, 67.38; H, 8.65. ¹H NMR (C₆D₆): δ 1.13 [m, 4H, {THF}], 1.58 [s, 18H, {–CMe₃}], 3.40 [m, 4H, {THF}], 6.82 [t, 1H, {4-H}], 7.30 [d, 2H, {3, 5-H}]. ¹³C {H} NMR(C₆D₆): δ 25.26 {THF}, 31.6 {–CMe₃}, 35.6 {–CMe₃}, 70.1 {THF}, 117.4 {4-C₆H₃}, 125.4 {3,5-C₆H₃}, 139.2 {2,6-C₆H₃}, 163.8 {*ipso*-C₆H₃}.

[(2,4,6-Trimethylphenoxide)₂Zn]_n, 5. A 0.5-g (3.7 mmol) amount of anhydrous ZnCl₂ was combined with a 1.4-g (7.6 mmol) amount of sodium bis-trimethylsilyl amide, which was refluxed in diethyl ether as before. After removal of the sodium chloride, the addition of 1.3 g (9.6 mmol) of 2,4,6-trimethylphenol resulted in the immediate precipitation of 1.0 g (56% yield) of polymeric product. Anal. Calcd for C₁₈H₂₂O₂Zn: C, 64.39; H, 6.60. Found: C, 63.80; H, 6.90.

Preparation and Isolation of Zinc(bis-trimethylsilyl amide), Zn-[N(SiMe₃)₂]₂. Alternatively, the synthesis of these bis phenoxides of zinc can be accomplished in a stepwise manner. That is, the Zn-[N(SiMe₃)₂]₂ intermediate can be isolated and purified in sizable quantities¹² and subsequently employed in the preparation of a variety of bis(phenoxide)ZnL₂ (L = base) derivatives.

In a drybox, anhydrous zinc chloride (5.0 g, 36.7 mmol) was placed in a 100-mL Schlenk flask along with approximately 2 equiv of NaN-(SiMe₃)₂ (12.1 g, 66.1 mmol). The flask was removed from the drybox and placed under a positive pressure of argon. Diethyl ether (60–70 mL) was added to the flask, and the reaction mixture was stirred for 1 h under argon. (**NOTE: This reaction is exothermic, generating enough heat to boil the ether. Hence, the reaction flask should be connected**

(6) (a) Kruper, W. J.; Smart, D. J. (The Dow Chemical Co.). U.S. Patent 4,500,704, 1983. (b) Chen, L.-B. *Makromol. Chem., Macromol. Symp.* **1992**, 59, 75. (c) Yang, S.-Y.; Fang, X.-G.; Chen, L.-B. *Polym. Adv. Technol.* **1996**, 7, 605.

(7) Sun, H.-N. (Arco Chemical Co.). U.S. Patent 4,783,445, 1988.

(8) (a) Super, M.; Berluce, E.; Costello, C.; Beckman, E. *Macromolecules* **1997**, 30, 368. (b) Super, M.; Beckman, E. J. *Macromolecular Symposia* **1998**, 127, 89.

(9) Darensbourg, D. J.; Holtcamp, M. W. *Macromolecules* **1995**, 28, 7577.

(10) Pray, A. R. *Inorg. Synth.* **1957**, 5, 153.

(11) Geerts, R. L.; Huffman, J. C.; Caulton, K. G. *Inorg. Chem.* **1986**, 25, 1803.

(12) Burger, H.; Sawodny, W.; Wannagat, U. *J. Organomet. Chem.* **1965**, 3, 113.

Table 1. Crystallographic Data for Complexes **1–4**, **6**, and **7**.

	1	2	3	4	6	7
formula	C ₄₄ H ₄₆ O ₄ Zn	C ₄₄ H ₄₂ O ₄ Zn	C ₃₂ H ₅₀ O ₄ Zn	C ₃₆ H ₅₈ O ₄ Zn	C ₃₆ H ₅₄ O ₈ Zn	C ₂₈ H ₃₂ N ₂ O ₂ Zn
formula weight	704.18	700.15	564.09	620.19	680.16	493.93
cryst system	orthorhombic	triclinic	monoclinic	monoclinic	orthorhombic	monoclinic
space group	<i>Ab</i> a2	<i>P</i> 1	<i>C</i> c	<i>P</i> 2 ₁ / <i>c</i>	<i>Ab</i> a2	<i>C</i> 2/ <i>c</i>
<i>a</i> , Å	19.851(13)	8.778(3)	24.079(7)	17.359(2)	21.688(9)	16.517(3)
<i>b</i> , Å	15.122(10)	11.348(4)	9.973(2)	10.1645(12)	9.622(3)	25.558(5)
<i>c</i> , Å	12.424(6)	19.078(6)	14.828(4)	20.981(6)	16.897(6)	14.638(3)
α , deg		77.87(3)				
β , deg	90	81.74(3)	120.57(2)	113.02(2)	90	121.16(3)
γ , deg		72.94(2)				
<i>V</i> , Å ³	3730(4)	1769.4(10)	3065.9(14)	3407.2(11)	3526(2)	5288(2)
<i>Z</i>	4	2	4	4	4	8
<i>d</i> (calcd), g/cm ³	1.254	1.314	1.222	1.209	1.281	1.241
absorp coeff, mm ⁻¹	0.700	0.737	0.834	0.756	0.745	0.954
no. of total reflections	1653	6621	1771	3927	1616	4094
no. of unique reflections	1653	6279	1767	3720	1616	3942
<i>R</i> , ^a %	4.90	6.81	2.96	6.10	8.33	6.91
<i>R</i> _w , ^a %	5.15	14.71	6.07	12.98	17.08	17.43

$$^a R = \sum ||F_o| - |F_c|| / \sum F_o. R_w = \{[\sum w(F_o^2 - F_c^2)^2] / [\sum w(F_o^2)^2]\}^{1/2}.$$

to a water-cooled condenser which is vented.) Upon cooling of the mixture to ambient temperature, NaCl precipitated out and was removed by filtration through a glass frit under an inert atmosphere. The solid collected was washed with two portions of ether (5 mL), and the combined ether filtrate was evaporated at reduced pressure to provide a clear, colorless oil of Zn[N(SiMe₃)₂]₂. The product was purified by vacuum distillation (2–3 mmHg) in a short-path apparatus at 103 °C; 9.4 g of product was collected (74% yield) and shown to be pure by ¹H NMR (singlet at 0.5 ppm).

(2,6-Di-*tert*-butylphenoxide)₂Zn(propylene carbonate)₂, 6. Two milliliters of a toluene solution of 2,6-di-*tert*-butylphenol (0.21 g, 1.04 mmol) was added via cannula to a solution of Zn[N(SiMe₃)₂]₂ (0.20 g or 0.52 mmol in 2 mL of toluene) under an atmosphere of argon. The reaction solution was allowed to stir for 1 h at ambient temperature, followed by the addition of 1.04 mmol (89 μ L) of propylene carbonate (PC) which was degassed and added via a microliter syringe. Upon removal of the toluene solvent under vacuum, an oily residue remained which was washed with hexane to provide a fine white powder of **6** in 69% yield. ¹H NMR (C₆D₆): δ 0.38 (d, 3H, PC-*Me*), shifted 0.27 ppm upfield from free PC; 1.70 (s, 12H, *t*-Bu); 2.68 (dd, 1H, PC methylene), shifted 0.47 ppm upfield from free PC; 3.11 (dd, 1H, PC methylene), shifted 0.39 ppm upfield from free PC; 3.49 (sx, 1H, PC methine), shifted 0.36 ppm upfield from free PC; 6.80 (t, 1H, benzylic H); 7.32 (d, 2H, benzylic Hs). Infrared of ν (CO): THF (1813 cm⁻¹), toluene (1818 cm⁻¹). This peak is unshifted from that in free propylene carbonate. Anal. Calcd for C₃₆H₅₄O₈Zn: C, 63.57; H, 8.00. Found: C, 61.58; H, 7.74. Clear, colorless crystals of **6** were obtained from a concentrated toluene solution of the complex maintained at -20 °C.

(2,4,6-Trimethylphenoxide)₂Zn(pyridine)₂, 7. In a procedure analogous to that described above for the preparation of **6**, 0.20 g (0.52 mmol) of Zn[N(SiMe₃)₂]₂ and 0.14 g (1.04 mmol) of 2,4,6-trimethylphenol were mixed in diethyl ether. A white solid, assumed to be an aggregate of bis-2,4,6-trimethylphenoxide zinc containing bridging phenoxide ligands, precipitated immediately. The reaction mixture was stirred for about 45 min at ambient temperature. Upon addition of 84 μ L (1.04 mmol) of distilled pyridine to the reaction mixture, the zinc complex completely dissolved. Vacuum removal of all volatiles led to a waxy, white solid which redissolved upon addition of ether solvent. ¹H NMR (C₆D₆): δ 2.21 (s, CH₃ of phenolate); 2.38 (s, CH₃ of phenolate); 6.48 (t, H on C₅H₅N), shifted 0.22 ppm downfield from free C₅H₅N; 6.6–6.8 (benzylic protons); 8.49 (d, H on C₃H₅N), shifted 0.04 ppm upfield from free C₅H₅N. Clear, colorless crystals of **7** were obtained from a concentrated THF solution of the complex layered with hexane and maintained at -20 °C.

Copolymerizations of Epoxides and Carbon Dioxide. A typical copolymerization run was as follows: 0.125 g of the respective zinc bisphenoxide complex was dissolved in cyclohexene oxide and/or propylene oxide. We typically used 5–20 mL of epoxide in various amounts depending on the desired copolymer. The solution was loaded

via an injection port into a 300-mL autoclave which had previously been dried overnight under vacuum at 90 °C. The autoclave was then placed under 700–800 psi of carbon dioxide and heated to the appropriate temperature. After the allotted time (48–69 h), the autoclave was allowed to cool to room temperature, upon which the polymer was extracted. Unreacted monomer was removed by repeated precipitation of the polymer from a dichloromethane solution with methanol.

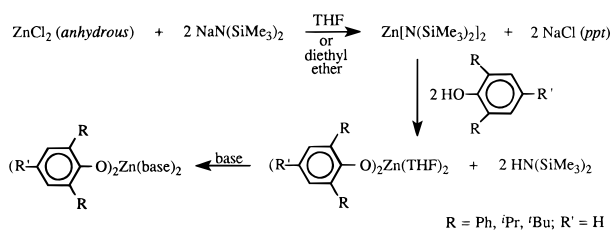
The insoluble catalyst, Zn(2,4,6-trimethylphenoxide)₂, was added to the reactor in the drybox. The reactor was then removed from the drybox, and the cyclohexene oxide was added through the injection port. The very reactive catalyst for homopolymerization of epoxides, Zn(2,4,6-tri-*tert*-butylphenoxide)₂(THF)₂, was sealed into a glass ampule and placed into the reactor. The reactor was evacuated overnight, and then the cyclohexene oxide was added via the injection port. The ampule was broken after the introduction of carbon dioxide and was heard to shatter upon stirring.

Variable-Temperature NMR Experiments. All variable-temperature experiments were performed using ¹H NMR on a 200E Varian instrument equipped with a variable-temperature unit. In a typical experiment, 20 mg of the desired Zn complex and 0.5 mL of CD₂Cl₂ were placed into an NMR tube, and the tube was sealed under vacuum. CD₂Cl₂ was replaced with benzene-*d*₆ for high-temperature experiments. Further information concerning individual experiments is discussed in the Results section.

Polymer Characterization. Polymer samples were first analyzed by means of IR and NMR spectroscopy for the absence of cyclic carbonates (ν (CO) = 1800 cm⁻¹) and percentages of ether and carbonate linkages (¹H: 3.45 and 4.60 ppm respectively). ¹H NMR was also used to check for the presence of cyclohexene oxide, which has a distinct singlet at 3.13 ppm. ¹³C NMR was utilized for determining the stereoregularity or tacticity of the polymer. *M*_w and *M*_n determinations were carried out by Exxon Research using GPC. Finally, trans stereochemistry was determined to be present in the polymer through a cleavage reaction. This was accomplished by refluxing a sample of the polymer in a methanolic solution of NaOH (2 g in 8 mL), according to the procedure described in the literature.^{3b} After the mixture was refluxed overnight, the solution was neutralized with hydrochloric acid and analyzed by GC/MS.

X-ray Crystallographic Studies of Complexes 1–4, 6, and 7. Crystal data and details of the data collection are provided in Table 1. Colorless block crystals of the six complexes were mounted on a glass fiber with epoxy cement at ambient temperature, and complexes **2** and **4** were cooled to 163 and 193 K, respectively, in a N₂ cold stream. Preliminary examination and data collection were performed on a Siemens P4 X-ray diffractometer (Mo K α , λ = 0.710 73 Å radiation). Cell parameters were calculated from the least-squares fitting of the setting angles for 25 reflections. ω scans for several intense reflections indicated acceptable crystal quality. Data were collected for 4.0° \leq 2θ \leq 50.0°. Three control reflections collected for every 97 reflections

Scheme 1



showed no significant trends. Background measurements by stationary-crystal and stationary-counter techniques were taken at the beginning and end of each scan for half of the total scan time. Lorentz and polarization corrections were applied to the total reflections for each complex listed in Table 1. A semiempirical absorption correction was applied to all complexes. Totals of unique reflections for each complex (Table 1) with $|I| \geq 2.0\sigma_I$ were used in further calculations. Structures were solved by direct methods [SHELXS, SHELXTL-PLUS program package, Sheldrick (1993)]. Full-matrix least-squares anisotropic refinement for all non-hydrogen atoms yielded R , $R_w(F^2)$, and S values at convergence for all complexes listed in Table 1. Hydrogen atoms were placed in idealized positions with isotropic thermal parameters fixed at 0.08. Neutral atom scattering factors and anomalous scattering correction terms were taken from the *International Tables for X-ray Crystallography*.¹³

Results and Discussion

Synthesis, Spectral, and Structural Characterization of Monomeric Zinc Phenoxides. The monomeric zinc phenoxide derivatives were synthesized in good, purified yields (50–80%) by the general synthetic route described by Caulton and co-workers¹¹ for the synthesis of the $(\text{ArO})_2\text{Zn}(\text{THF})_2$ complexes, where $\text{OAr} = 2,4,6\text{-tri-}t\text{-butylphenoxide}$ and $2,6\text{-di-}t\text{-butylphenoxide}$. We have performed the process outlined in Scheme 1 both in a one-pot synthesis and by isolating/purifying the $\text{Zn}[\text{N}(\text{SiMe}_3)_2]_2$ intermediate prior to its reaction with the various phenols. It is important to remove the NaCl precipitant formed in the initial step prior to carrying out the subsequent acid–base reaction in order to avoid the formation of complexes which incorporate sodium chloride, e.g., $\text{Na}[(2,6\text{-diisopropylphenoxide})_4\text{Zn}_2\text{Cl}]\cdot 3\text{THF}$.¹⁴ The X-ray structure of this dimeric species shows the sodium ion to be six-coordinate, involved in an η^6 -interaction with the phenoxide π -system, and bound to two THF ligands and a zinc-bridged chloride ligand. In the instance of $\text{R} = \text{R}' = \text{Me}$, i.e., the 2,4,6-trimethylphenol-derived product, the zinc complex immediately precipitates out of solution. This behavior is indicative of aggregate formation in the absence of steric inhibition by this less bulky phenoxide ligand. However, the aggregation, which presumably involves bridging phenoxide ligands, is readily disrupted by strong bases such as pyridine to afford monomeric, soluble adducts.

As illustrated in Scheme 1, the ether ligands upon isolation of these zinc complexes can be replaced by other bases; e.g., the relevant bases for the studies reported herein include epoxides, propylene carbonate, pyridine, and phosphines.¹⁵ The propylene oxide derivative was prepared by repeated dissolution of the diethyl ether complex in the epoxide solvent. Unfortunately, we have not yet been able to isolate and fully characterize an epoxide complex of zinc as we have been able to accomplish for the other adducts (vide infra). This, in part, is due to the

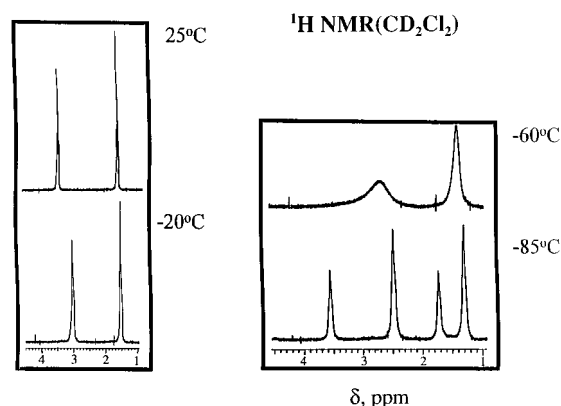


Figure 1. Variable-temperature ^1H NMR spectra of (2,6-diphenylphenoxide) $\text{Zn}(\text{THF})_2$ (**2**) dissolved in CD_2Cl_2 in the THF region of the spectrum.

weak binding ability of epoxides as ligands. Indeed, in the base adducts of $\eta^3\text{-HB}(3\text{-Phpz})_3\text{Cd}(\text{acetate})$, we have quantified the order of ether binding as $\text{THF} > \text{dioxane} > \text{cyclohexene oxide} \geq \text{propylene oxide}$.¹⁶ On the other hand, in the case involving the zinc phenoxide derivative containing 2,6-*tert*-butyl substituents, homopolymerization of the epoxide occurred rapidly at ambient temperature, thereby prohibiting the isolation of an epoxide adduct.

Although the solid-state structures of these monomeric zinc phenoxides all reveal coordination of the various bases to the zinc center (vide infra), in solution the extent of base binding is greatly dependent on the temperature, solvent, base, and nature of phenoxide ligands coordinated to zinc. For example, upon dissolving (2,6-diphenylphenoxide) $\text{Zn}(\text{THF})_2$ (**2**) in C_6D_6 or CD_2Cl_2 , the THF ligands are essentially completely dissociated from the metal center at ambient temperature, as demonstrated by ^1H NMR spectroscopy. That is, the proton resonances for the $\alpha\text{-CH}_2$ and $\beta\text{-CH}_2$ groups of THF in the case of complex **2** dissolved in CD_2Cl_2 occur at 3.46 and 1.72 ppm, respectively, whereas the corresponding resonances are observed at 3.69 and 1.83 ppm for free THF in CD_2Cl_2 . Similarly, at ambient temperature, these proton resonances are observed at 3.53 and 1.39 ppm for complex **2** dissolved in C_6D_6 compared to 3.55 and 1.43 ppm for free THF in C_6D_6 . Upon lowering the temperature of a CD_2Cl_2 solution of **2**, the two ^1H resonances assigned to THF shifted upfield and between -40 and -60 $^\circ\text{C}$ are seen to broaden. Eventually, four resonances at 3.57 and 1.73 ppm (free THF)¹⁷ and 2.49 and 1.30 ppm (bound THF) appeared at -85 $^\circ\text{C}$, indicative of slow THF exchange (Figure 1). Unlike what is seen in the 2,6-di-*tert*-butylphenoxide analogue (vide infra), complex **4**, the $\alpha\text{-CH}_2$ protons are shifted upfield to a greater extent than the $\beta\text{-CH}_2$ units, as anticipated for coordination of the oxygen atom of THF to the zinc center, where the CH_2 unit closest to the donor atom should experience the larger change in electronic environment.

As noted in Figure 1, not all of the THF ligands are bound to the zinc center at -85 $^\circ\text{C}$ in complex **2**.¹⁸ Nevertheless, from the integrated peak intensities, the ratio of bound to free THF is greater than 1. Indeed, in the instance where the total THF to

(16) Darensbourg, D. J.; Niezgoda, S. A.; Holtcamp, M. W.; Draper, J. D.; Reibenspies, J. H. *Inorg. Chem.* **1997**, *36*, 2426.

(17) There is a small upfield shift of the free THF proton resonances in CD_2Cl_2 as the temperature is lowered from ambient to -85 $^\circ\text{C}$ of 0.12 and 0.10 ppm.

(18) Upon evacuating samples of the bisphenoxide complexes of zinc at reduced pressures at ambient temperature, some THF is lost from the isolated solid. That is, the ratio of THF to zinc is less than 2:1, generally being about 1.8:1 if evacuation is not carried out for a prolonged period.

(13) Ibers, J. A.; Hamilton, W. C., Eds. *International Table for X-ray Crystallography*; Kynoch Press: Birmingham, England, 1974; Vol. IV.

(14) Darensbourg, D. J.; Yoder, J. C.; Struck, G. E.; Holtcamp, M. W.; Draper, J. D.; Reibenspies, J. H. *Inorg. Chim. Acta* **1998**, *274*, 115.

(15) Darensbourg, D. J.; Zimmer, M. S.; Rainey, P.; Larkins, D. L. *Inorg. Chem.* **1998**, *37*, 2852.

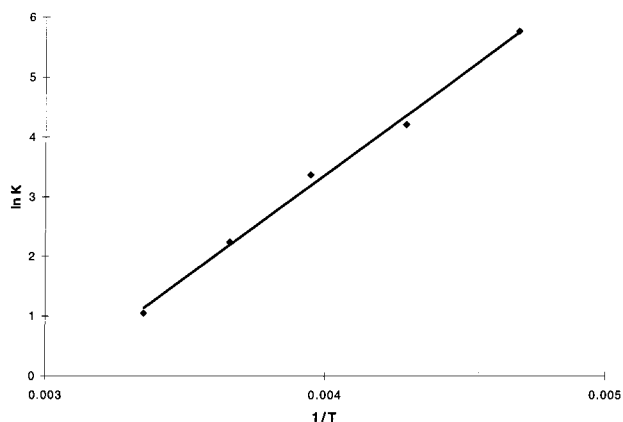
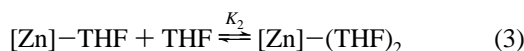
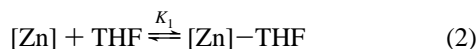


Figure 2. Logarithmic plot of K_f as a function of temperature for complex **2** in CD_2Cl_2 solution.

zinc molar ratio was determined to be 1.8, the bound THF to zinc ratio at -85°C was shown to be 1.4. Hence, the facile stepwise equilibria (eqs 2 and 3) which exist between free and bound THF bases lie intermediate between the (2,6-diphenylphenoxide) $_2\text{Zn}(\text{THF})$ and (2,6-diphenylphenoxide) $_2\text{Zn}(\text{THF})_2$ species.¹⁹ From the fast-exchange region of the ^1H NMR spectra



$$K_f = \frac{\{[\text{Zn}]-(\text{THF})_2\}}{\{[\text{Zn}]\}\{\text{THF}\}^2},$$

where $[\text{Zn}] = (2,6\text{-diphenylphenoxide})_2\text{Zn}$

(between 25 and -60°C), the overall formation constant ($K_f = K_1K_2$) can be determined as a function of temperature according to the method of Popov.²⁰ From the linear relationship of $\ln K_f$ vs T^{-1} (Figure 2) for the composite equilibrium defined in eqs 2 and 3, the values of ΔH° , ΔS° , and ΔG° were calculated to be -28.9 kJ/mol, -87.4 J/mol, and -2.80 kJ/mol, respectively. The complex formation constant (K_f) was found to be 2.86 at 25°C . In addition, from the estimated rates of THF exchange (40 s^{-1} at -75°C) as a function of temperature, an E_a value of 44 kJ/mol was obtained.

The effect of changing the electron-withdrawing 2,6-diphenyl substituents on the phenoxide ligands to the electron-releasing 2,6-di-*tert*-butyl groups leads to faster bound/free THF exchange rates. That is, starting with a sample of (2,6-di-*tert*-butylphenoxide) $_2\text{Zn}(\text{THF})_x$ (where $x = 1.2\text{--}1.4$) in toluene, it was not possible to observe the slow exchange limit at -80°C . The free/bound THF exchange rate is approximated to be greater than 200 s^{-1} at -80°C . It is important to reiterate here that, in this derivative, the $\beta\text{-CH}_2$ proton signal of the THF ligands shifts upfield to a much greater extent than the $\alpha\text{-CH}_2$ signal in toluene solution. A similar observation has previously been reported for this complex in benzene by Caulton and co-workers.¹¹ For the temperature range from 20 to -80°C , the proton resonances for the $\alpha\text{-CH}_2$ and $\beta\text{-CH}_2$ groups in THF shift from 3.339 and 1.064 ppm to 3.108 and 0.674 ppm, respectively, for the (2,6-di-*tert*-butylphenoxide) $_2\text{Zn}(\text{THF})_{1,2}$ in toluene.²¹ From the mag-

(19) It should be noted here that it is not possible to isolate the THF resonances for these individual zinc species at -85°C in CD_2Cl_2 .

(20) (a) Roach, E. T.; Hardy, P. R.; Popov, A. I. *Inorg. Nucl. Chem. Lett.* **1973**, *9*, 359. (b) Popov, A. I. In *Modern NMR Techniques and Their Application in Chemistry*; Popov, A. I., Hallenga, K., Eds.; Marcel Dekker: New York, 1987; p 485.

Table 2. Selected Bond Distances (\AA) and Bond Angles (deg) for Complexes **1–4**, **6**, and **7**^{a,b}

Complex 1: $\text{Zn}(\text{O}-2,6\text{-Ph}_2\text{C}_6\text{H}_3)_2(\text{Et}_2\text{O})_2$			
Zn(1)–O(1)	1.886(6)	Zn(1)–O(2)	2.107(7)
O(1)–C(1)	1.333(11)		
O(1)–Zn(1)–O(1A)	140.0(4)	C(1)–O(1)–Zn(1)	125.1(6)
O(1)–Zn(1)–O(2)	103.5(3)	O(2)–Zn(1)–O(2A)	94.6(4)
O(1)–Zn(1)–O(2A)	103.3(3)	Zn(1)–O(2)–[OC ₂ plane]	168.0(4)
Complex 2: $\text{Zn}(\text{O}-2,6\text{-Ph}_2\text{C}_6\text{H}_3)_2(\text{THF})_2$			
Zn(1)–O(1)	1.864(4)	Zn(1)–O(2)	1.864(4)
Zn(1)–O(3)	2.080(4)	Zn(1)–O(4)	2.036(4)
O(1)–C(1)	1.335(6)	O(2)–C(19)	1.332(6)
O(1)–Zn(1)–O(2)	136.2(2)	O(1)–Zn(1)–O(3)	106.5(2)
O(1)–Zn(1)–O(4)	106.6(2)	O(2)–Zn(1)–O(4)	108.5(2)
O(4)–Zn(1)–O(3)	90.5(2)	C(1)–O(1)–Zn(1)	122.3(3)
Zn(1)–O(3)–[OC ₂ plane]	168.8(4)	C(19)–O(2)–Zn(1)	133.0(4)
		Zn(1)–O(4)–[OC ₂ plane]	174.4(3)
Complex 3: $\text{Zn}(\text{O}-2,6\text{-}^i\text{Pr}_2\text{C}_6\text{H}_3)_2(\text{THF})_2$			
Zn(1)–O(1)	1.846(11)	Zn(1)–O(2)	1.856(13)
Zn(1)–O(3)	2.028(13)	Zn(1)–O(4)	2.074(11)
O(1)–C(1)	1.29(2)	O(2)–C(13)	1.38(2)
O(1)–Zn(1)–O(2)	139.8(2)	O(1)–Zn(1)–O(3)	106.0(5)
O(1)–Zn(1)–O(4)	104.2(5)	O(2)–Zn(1)–O(4)	103.9(5)
O(4)–Zn(1)–O(3)	91.0(2)	C(1)–O(1)–Zn(1)	127.0(11)
Zn(1)–O(3)–[OC ₂ plane]	174.0(3)	C(13)–O(2)–Zn(1)	124.3(10)
		Zn(1)–O(4)–[OC ₂ plane]	172.3(3)
Complex 4: $\text{Zn}(\text{O}-2,6\text{-}^i\text{Bu}_2\text{C}_6\text{H}_3)_2(\text{THF})_2$			
Zn(1)–O(1)	1.873(5)	Zn(1)–O(2)	1.878(5)
Zn(1)–O(3)	2.103(5)	Zn(1)–O(4)	2.086(7)
O(1)–C(1)	1.348(8)	O(2)–C(15)	1.360(8)
O(1)–Zn(1)–O(2)	142.9(2)	O(1)–Zn(1)–O(3)	104.3(2)
O(1)–Zn(1)–O(4)	101.1(2)	O(2)–Zn(1)–O(4)	99.6(2)
O(4)–Zn(1)–O(3)	100.3(2)	C(1)–O(1)–Zn(1)	134.2(5)
Zn(1)–O(3)–[OC ₂ plane]	174.0(2)	C(15)–O(2)–Zn(1)	131.0(4)
		Zn(1)–O(4)–[OC ₂ plane]	175.5(4)
Complex 6: $\text{Zn}(\text{O}-2,6\text{-}^i\text{Bu}_2\text{C}_6\text{H}_3)_2(\text{PC})_2$			
Zn(1)–O(1)	1.850(11)	Zn(1)–O(2)	2.071(11)
O(1)–C(1)	1.30(2)	O(2)–C(15)	1.20(2)
O(1)–Zn(1)–O(1A)	136.4(7)	C(1)–O(1)–Zn(1)	155.7(10)
O(1)–Zn(1)–O(2)	100.4(5)	O(2)–Zn(1)–O(2A)	96.3(6)
O(1)–Zn(1)–O(2A)	108.4(5)	Zn(1)–O(2)–C(15)	127.5(13)
Complex 7: $\text{Zn}(\text{O}-2,4,6\text{-Me}_3\text{C}_6\text{H}_3)_2(\text{Py})_2$			
Zn(1)–O(1)	1.885(4)	Zn(1)–N(1)	2.065(5)
O(1)–C(1)	1.330(8)		
O(1)–Zn(1)–O(1A)	134.5(3)	O(1)–Zn(1)–N(1)	103.3(2)
O(1)–Zn(1)–N(1A)	104.8(2)	C(1)–O(1)–Zn(1)	136.5(4)
N(1)–Zn(1)–N(1A)	102.2(3)		

^a Estimated standard deviations are given in parentheses. ^b Symmetry-generated atoms designated by (#A).

nitude of these upfield proton shifts of the THF ligand in this derivative, 0.211 and 0.366 ppm, there is significant THF binding even at ambient temperature. As expected in excess THF, where the THF:Zn ratio is equal to 4.2, these proton signals appear much closer to those of free THF at 3.521 and 1.219 ppm at 20°C . Hence, the K_f values for the equilibria defined in eqs 2 and 3 are greater in this instance than those for the 2,6-diphenylphenoxide derivative. *The order of ligand binding as a function of the nature of the phenoxide ligands is seen in other instances for both zinc and cadmium derivatives encompassing a wide variety of ligands.*^{15,22} *This trend in metal–ligand binding most likely reflects the greater steric requirements of the 2,6-diphenyl ligands. Based on electronic arguments, the opposite effect would be anticipated, i.e., metal–ligand binding would be enhanced by electron-withdrawing substituents on the phenolate ligands.*

Complexes **1–4**, **6**, and **7** have been characterized in the solid state by X-ray crystallography, and a list of selected bond lengths and angles is provided in Table 2. All complexes crystallize as

(21) There is a small upfield shift of the $\beta\text{-CH}_2$ proton resonance of free THF in toluene of 0.13 ppm at -80°C .

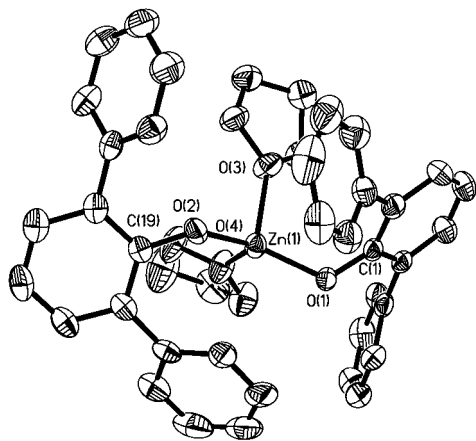


Figure 3. Molecular structure of complex **2**; thermal ellipsoids at 50% probability.

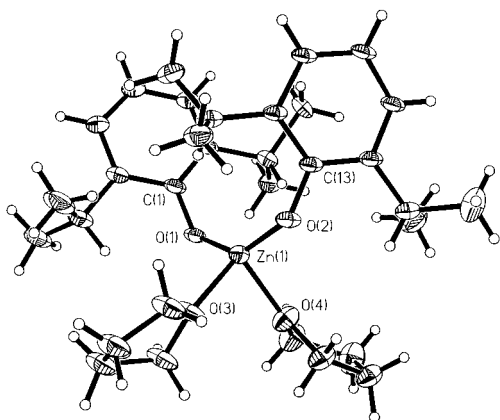


Figure 4. Molecular structure of complex **3**; thermal ellipsoids at 50% probability.

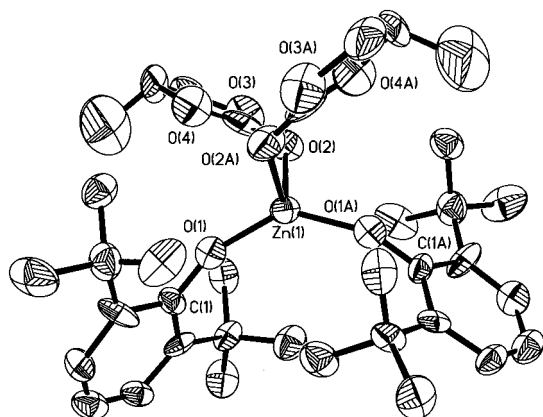


Figure 5. Molecular structure of complex **6**; thermal ellipsoids at 50% probability.

four-coordinate monomers with highly distorted tetrahedral geometry about the zinc center, much like that exhibited by the originally reported analogue, (2,4,6-tri-*tert*-butylphenoxy)₂Zn-(THF)₂ (**8**).¹¹ Thermal ellipsoid representations of selected derivatives may be found in Figures 3–5, along with a common abbreviated atom labeling scheme (other figures may be found in the Supporting Information). The skeletal rendition, indicating the salient solid-state structural features of these derivatives, is displayed in Scheme 2. In all instances, the angle between the two sterically encumbering phenoxy ligands (θ) is significantly more obtuse than the corresponding angles observed between the two smaller neutral base ligands (ϕ). For example, the values of θ in complexes **1–4** and **6** span the narrow range of 136.2–

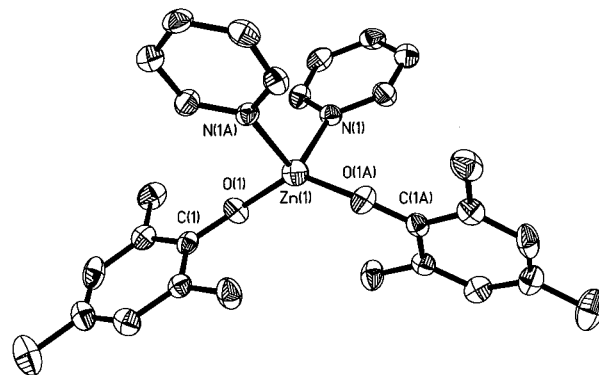
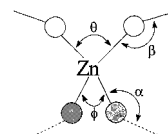


Figure 6. Molecular structure of complex **7**; thermal ellipsoids at 50% probability.

Scheme 2



142.9°, whereas the corresponding values encompassed by ϕ are 90.5–100.3°. Interestingly, the structures of the closely related derivatives, **4** and **8**,¹¹ which differ only in the presence of a *tert*-butyl substituent in the 4-position of the phenoxy ring in the latter case, have strikingly different θ parameters (142.9-(2)° vs 121.7(3)°) with more comparable ϕ values (100.3(2)° vs 94.93(27)°). For the sterically less bulky 2,4,6-trimethylphenoxy derivative, which is insoluble in ether solvents but solubilized upon addition of 2 equiv of the better donor ligand pyridine and crystallized as complex **7**, the θ angle of 134.5° is quite similar to those found in the other derivatives. The thermal ellipsoid drawing of **7** is displayed in Figure 6, where the N–Zn–N angle, analogous to ϕ in the ether derivatives, was observed to be 102.2°.

The average Zn–O(aryl) bond distances in all of the structurally characterized zinc derivatives (complexes **1–4**, **6**, and **8**) which contain the O₄ core atom ligand set are quite similar, covering a range of only 0.037 Å, i.e., 1.850–1.887 Å. Similarly, Zn–O(aryl) bond lengths of 1.885(5) Å are seen in the pyridine adduct, complex **7**, where the O₂N₂ ligand set is present. Likewise, the Zn–O (THF, Et₂O, PC) bond length varies only slightly, from 2.051 to 2.107 Å, although these neutral ligands differ somewhat in donor properties. The Zn–N bond distance in **7** is 2.065(4) Å, consistent with a slightly stronger interaction and the 0.02 Å longer effective atomic radius of nitrogen as compared to oxygen. The average Zn–O–C(aryl) angles (β in Scheme 2) in all of these derivatives traverse the broad range of 125.1–155.7°. Interestingly, the oxygen donor ligand propylene carbonate in complex **6** is pyramidal, with a Zn–O–C angle (α) of 127.5(13)°, whereas the corresponding angles in the ether donor ligand derivatives (defined by the Zn–O vector and the midpoint of the OC₂ plane) are much more obtuse (168.0–175.5°). This latter observation presumably results from the ether donor's ability to accommodate the bulky phenoxy ligands. Indeed, this has previously been seen in the cadmium analogues.²²

Copolymerization Reactions of Epoxides and Carbon Dioxide. Because of the solution properties exhibited by the monomeric (phenoxy)₂Zn(ether)₂ derivatives described in this report, it is expected that these complexes should serve as good

(22) Darensbourg, D. J.; Niezgod, S. A.; Draper, J. D.; Reibenspies, J. H. *J. Am. Chem. Soc.* **1998**, *120*, 4690.

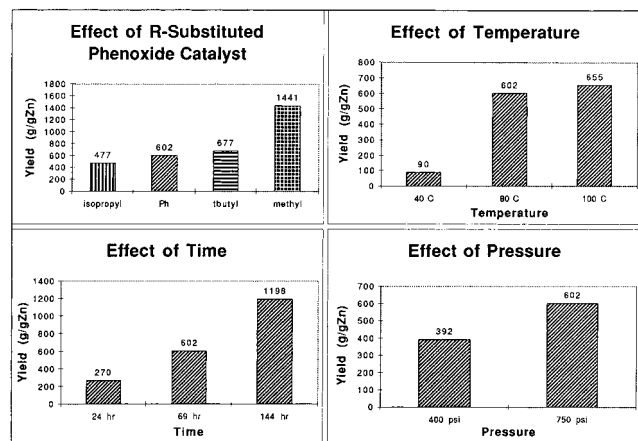


Figure 7. Yield of copolymer (cyclohexene oxide/CO₂) in g/g of Zn for a 69 h run at 80 °C and 750 psi loading pressure of CO₂ using various bis(phenoxide)₂Zn complexes, and effects of reaction conditions on copolymer yield employing the (2,6-diphenylphenoxide)₂Zn(Et₂O)₂ (1) catalyst.

catalysts or catalyst precursors for ring-opening of epoxides and CO₂ coupling processes. This should be particularly true in *noninteracting solvents*, where there would be little competition for metal binding of the weakly interacting epoxide substrates. Indeed, we have communicated preliminary results demonstrating the efficiency of these complexes for catalyzing the copolymerization process defined in eq 4, where $m \gg n$.⁹ Herein, we wish to describe these studies in greater detail.

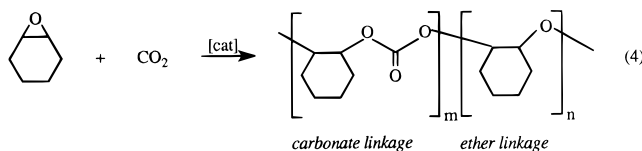


Figure 7 (top-left corner) summarizes the effect of R substituents on the phenoxide ligands of the zinc(ether)₂ complexes on the yield of high-molecular-weight polymer (characterized by its insolubility in methanol) for the copolymerization reaction defined in eq 4. *It is important to note here that these processes were carried out in the absence of added solvents; i.e., the reactants, zinc phenolates/cyclohexene oxide/CO₂ constitute the reaction system.* Furthermore, prior to the production of large quantities of copolymers under the reaction conditions specified, the solutions appeared to be homogeneous, as evidenced by a video recording of processes performed in a high-pressure reactor equipped with sapphire windows. As indicated in Figure 7, the yield of high-molecular-weight polymer increases over a reaction period of 69 h from 477 to 1441 g of polymer/g of zinc as the substituents on the phenolate ligands of the catalyst vary as ⁱPr < Ph < ^tBu < Me. Also described in Figure 7 are the effects of time, temperature, and pressure on the polymer yield for the (2,6-diphenylphenoxide)₂Zn-(Et₂O)₂ catalyst system. The polymer yield was not enhanced for a reaction carried out at much higher pressures of carbon dioxide, i.e., supercritical conditions.²³ The 2,6-di-*tert*-butylphenoxide derivative, complex 4, was very active as an epoxide homopolymerization catalyst to afford high-molecular-weight polyethers. To retard this process relative to copolymerization,

(23) For a polymer run carried out with complex 2 as catalyst at 80 °C and 6500 psi of CO₂ (thanks to Dr. Christine Costello at Exxon Research, Annandale), the yield (357 g/g of Zn) and % carbonate linkages (90) of copolymer were essentially identical to those of an otherwise analogous run performed at 80 °C and 800 psi pressure (366 g/g of Zn and 91% carbonate linkages).

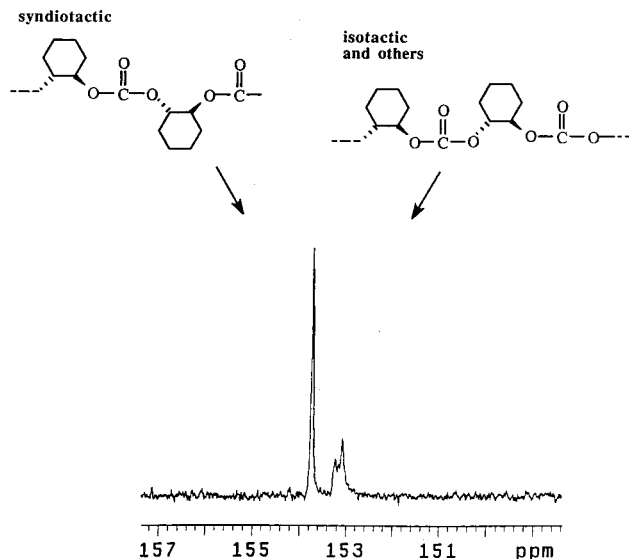


Figure 8. ¹³C NMR spectrum of poly(cyclohexene carbonate) obtained with complex 5 as catalyst. Recorded in CDCl₃ at ambient temperature.

it was necessary to initially pressurize the cyclohexene oxide loaded reactor with CO₂ prior to introducing the catalyst. This was accomplished by placing the catalyst in a sealed glass ampule which was broken when mechanical stirring was started.²⁴

The polymers were characterized by FTIR and ¹H and ¹³C NMR spectroscopies utilizing the previously established methodology for similar copolymers produced from other zinc catalyst systems.²⁵ The intense asymmetric $\nu(\text{CO}_2)$ stretching vibration of the polycarbonate linkages was observed at 1750 cm⁻¹. The percentage of carbonate linkage in the purified polymer was calculated from the relative intensities of the ¹H NMR signals of the methine protons next to the carbonate linkages ($\delta = 4.60$ ppm) and ether linkages ($\delta = 3.45$ ppm). In general, the carbonate linkages were greater than 90% for reactions carried out at CO₂ pressures greater than 750 psi. A notable exception, where carbonate linkages were as low as 53%, was observed for the very active epoxide homopolymerization catalyst, (2,6-di-*tert*-butylphenoxide)₂Zn(THF)₂. ¹³C NMR spectroscopy in the carbonate region was utilized to assess the stereoregularity or tacticity of the polymer (Figure 8). That is, consistent with previous reports,²⁵ there are two ¹³C resonances at $\delta = 153.7$ and 153.1 ppm which are assigned to syndiotactic and isotactic copolymer chain tacticity on the basis of corresponding ¹³C NMR data from the model compound 2,2'-oxydicyclohexanol.²⁶ In addition, there is at least one more carbonate ¹³C resonance at 153.3 ppm which can be assigned to heterotactic forms of the copolymer. As is readily apparent from Figure 8, the copolymer chain tacticity is predominantly *syndiotactic*. The stereochemistry of the cyclohexene oxide ring-opening reaction in the cyclohexene oxide/carbon dioxide

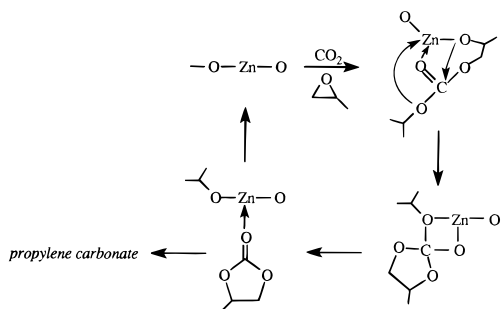
(24) Alternatively, we have recently shown that the rate of the homopolymerization of cyclohexene oxide catalyzed by complex 4 is greatly retarded in the presence of 1 equiv of PCy₃, where the complex (2,6-di-*tert*-butylphenoxide)₂ZnPCy₃ is formed at ambient temperature.¹⁵ At the same time, the copolymerization process readily occurs; e.g., under the reaction conditions defined in Figure 7, where complex 4 provides 677 g of polymer/g of Zn with *only* 53% carbonate linkages, this catalyst in the presence of 1 equiv of PCy₃ affords 375 g of polymer/g of Zn with over 92% carbonate linkages. A more definitive study of phosphine derivatives of zinc and cadmium phenoxides and their role in copolymerization catalysis of epoxides and CO₂ will be the subject of a later publication.

(25) (a) Kuran, W.; Listos, T. *Macromol. Chem. Phys.* **1994**, *195*, 977.

(b) Koinuma, H.; Hirai, H. *Makromol. Chem.* **1977**, *178*, 1283.

(26) Hasebe, Y.; Tsuruta, T. *Makromol. Chem.* **1987**, *188*, 1403.

Scheme 3



copolymerization processes was determined to be trans by alkaline hydrolysis of the polymer, which provided pure *trans*-1,2-cyclohexanediol.²⁷ The molecular weights (M_n and M_w) of the methanol-insoluble copolymers were measured by gel permeation chromatography (GPC) by comparison with polystyrene standards, with M_w values ranging from 45×10^3 to 173×10^3 and M_w/M_n ratios varying from 2.5 to 4.5. However, the polydispersity indexes have been observed to be as large as 10 in a few catalytic runs. This broad range in polydispersity may be attributed to more than one zinc species initiating the polymerization process or to protonation being the termination step. It is estimated, based on M_n and the yield of polymer, that greater than 50% of the zinc atoms are active in forming high-molecular-weight copolymers.

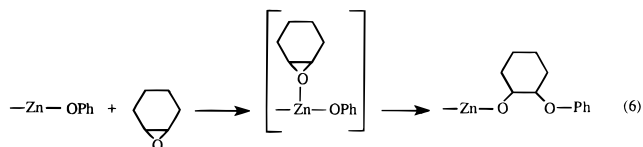
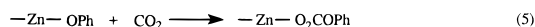
Under the reaction conditions where these zinc phenolates actively catalyze the copolymerization of cyclohexene oxide and carbon dioxide, the reaction between propylene oxide and CO_2 leads predominantly to *propylene carbonate*. This process presumably occurs via the back-biting reaction depicted in Scheme 3.^{25a} This observation is in agreement with results from other laboratories, where in the absence of steric constraints about the metal center the back-biting process is favored over polymer growth when propylene oxide is the substrate. Nevertheless, at much lower temperatures (e.g., 40 °C using complex **2** as catalyst), copolymer formation is slightly favored over cyclic carbonate production. Evidently, the rate of cyclic carbonate formation has a greater temperature dependence than the rate of copolymer production. Furthermore, the ratio of cyclic carbonate to copolymer afforded at these low temperatures is influenced to a small extent by the substituents on the phenoxide complex employed as catalyst.

On the contrary, the terpolymerization reaction between cyclohexene oxide/propylene oxide/ CO_2 readily takes place in the presence of these zinc phenolate catalysts, with little cyclic carbonate production at low propylene oxide loadings (<50% mole fraction). As anticipated on the basis of similar affinity of the group 12 metals for the two epoxides,¹⁶ the resulting terpolymer is a random mixture of polycarbonate linkages with small quantities of polyether linkages. The ^{13}C NMR spectra of these terpolymers (reported in ref 9) display, in addition to isotactic and syndiotactic poly(cyclohexenylene carbonate) linkages, head-to-tail and tail-to-tail poly(propylene carbonate) linkages.²⁸ Other less intense carbonate resonances assignable to some combination of various cyclohexenylene carbonate-propylene carbonate linkages were also present in the spectra. The lack of cyclic propylene carbonate formation during this process is attributed to steric encumbrance provided by the cyclohexene carbonate linkages which inhibit the process in a

manner analogous to that depicted in Scheme 3 for propylene oxide/ CO_2 copolymerization.

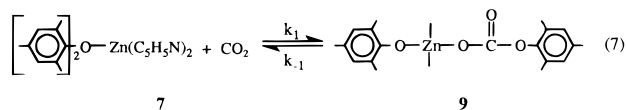
Relevant to the zinc-bound propylene carbonate intermediate indicated in Scheme 3, it is of importance to note that propylene carbonate is a much better ligand toward zinc than cyclic ethers. That is, in this investigation, propylene carbonate was found to be bound to zinc when complex **6** was dissolved in C_6D_6 at ambient temperature by ^1H NMR spectroscopy. All proton resonances for the propylene carbonate ligand in complex **6** are shifted significantly upfield; e.g., the multiplet for the hydrogen attached to the carbon bearing the CH_3 group is shifted from 3.93 ppm in free propylene carbonate to 3.46 ppm. Furthermore, the addition of excess THF to a benzene solution of **6** did not alter the propylene carbonate binding. Hence, the stronger affinity of zinc for propylene carbonate, a byproduct of the copolymerization process, over cyclic ethers (particularly epoxides) should greatly inhibit these catalytic reactions.

Carbon Dioxide Insertion Reactions Involving Zinc Phenoxides. It is of interest to examine the insertion reaction of carbon dioxide into the $\text{Zn}-\text{O}$ bond of these bis(phenoxide)Zn derivatives since, in the initiation process for the copolymer synthesis, CO_2 insertion (eq 5) and/or epoxide ring-opening (eq 6) could be occurring. The latter process requires prior substrate



coordination, whereas the CO_2 insertion process has been demonstrated in previous studies to be a concerted reaction.²⁹ Furthermore, we have demonstrated that the reaction depicted in eq 5 is greatly inhibited for bulky metal phenolates.³⁰ For example, CO_2 rapidly and reversibly inserts into the $\text{W}-\text{OPh}$ bond of the $\text{W}(\text{CO})_5\text{OPh}^-$ anion to afford $\text{W}(\text{CO})_5\text{O}_2\text{COPh}^-$, but insertion of CO_2 into the $\text{W}-\text{O}$ bond of (2,6-diphenylphenoxide) $\text{W}(\text{CO})_5^-$ does not occur, even at high pressures of CO_2 . That is, CO_2 insertion is governed by the accessibility of the oxygen lone pairs on the phenoxide for interaction with the weakly electrophilic carbon center of CO_2 . Herein we have examined the propensity for CO_2 insertion into a sterically encumbered vs sterically accessible metal phenoxide employing ^{13}C NMR spectroscopy.

Upon bubbling $^{13}\text{CO}_2$ into a pyridine- d_5 solution of complex **7**, (2,4,6-trimethylphenoxide) $_2\text{Zn}(\text{C}_5\text{H}_5\text{N})_2$, in addition to the broad peak for free $^{13}\text{CO}_2$, a ^{13}C resonance in the carbonate region at 170.1 ppm was evident (peak c in Figure 9B). Moreover, the ^{13}C signal corresponding to the *ipso* carbon of the phenoxide ring was split into two resonances, one at its original position (162.5 ppm, peak a) and one shifted downfield to 165.9 ppm (peak a* in Figure 9B). This latter observation is indicative of CO_2 insertion into only one of the metal phenolate groups (eq 7). In addition, from the relative peak intensities of



(27) Inoue, S.; Koinuma, H.; Yokoo, Y.; Tsuruta, T. *Makromol. Chem.* **1971**, *143*, 97.

(28) Lednor, P. W.; Rol, N. C. *J. Chem. Soc., Chem. Commun.* **1985**, 598.

(29) Darensbourg, D. J.; Sanchez, K. M.; Reibenspies, J. H.; Rheingold, A. L. *J. Am. Chem. Soc.* **1989**, *111*, 7094.

(30) Darensbourg, D. J.; Mueller, B. L.; Bischoff, C. J.; Chojnacki, S.; Reibenspies, J. H. *Inorg. Chem.* **1991**, *30*, 2418.

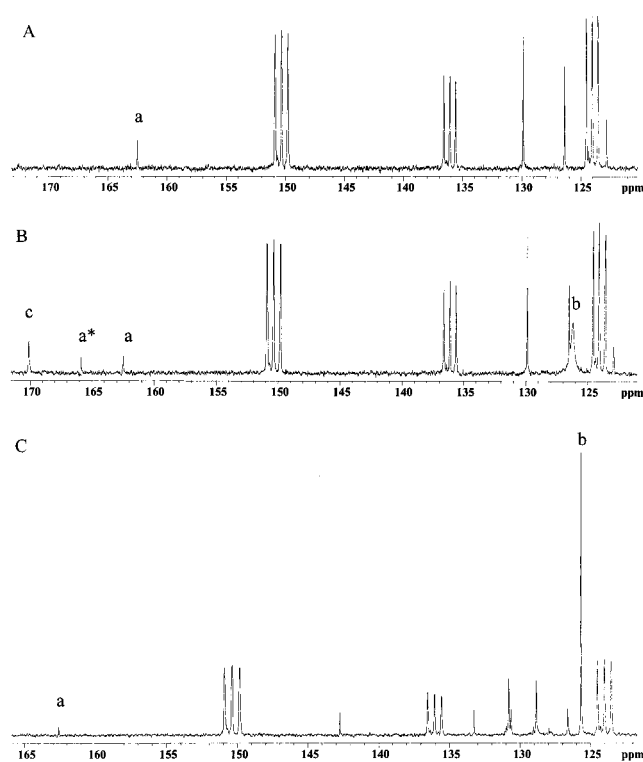


Figure 9. (A) ^{13}C NMR spectrum of complex **7** in $\text{C}_5\text{D}_5\text{N}$. (B) ^{13}C NMR spectrum of complex **7** in $^{13}\text{CO}_2$ saturated $\text{C}_5\text{D}_5\text{N}$. (C) ^{13}C NMR spectrum of complex **2** in $^{13}\text{CO}_2$ -saturated $\text{C}_5\text{D}_5\text{N}$.

the *ipso* carbon resonances (a and a*), which would be anticipated to have similar T_1 values, it is possible to conclude that the insertion reaction (eq 7) lies far to the right. Because complex **7** is four-coordinate in pyridine solution, as shown by ^1H NMR, the resulting carbonate derivative is most likely monomeric.³¹ This is to be contrasted with the dimer which has been isolated and structurally characterized from the reaction of (2,6-diphenylphenoxide)₂Cd(THF)₂ and CS_2 in benzene.²² Furthermore, the fact that CO_2 insertion readily occurs in the coordinating solvent pyridine is totally consistent with previous mechanistic aspects in general, where no prior coordination of CO_2 to the metal is necessary for C–O bond formation. At the same time, strongly interacting solvents render these complexes inert to ring-opening reaction (eq 6), where coordinating of substrates is required, i.e., homo- or copolymerization of epoxides does not take place in coordinating solvents. On the other hand, upon saturating a pyridene-*d*₅ solution of the sterically encumbered (2,6-diphenylphenoxide)₂ Zn derivative with $^{13}\text{CO}_2$, no reaction was observed (Figure 9C). This is similar to our observation previously reported for the cadmium analogue²² and in group 6 carbonyl derivatives.³⁰

The broadness and slight shift downfield (126.2 vs 125.7 ppm) of the free $^{13}\text{CO}_2$ peak for the reaction defined in eq 7 and depicted in Figure 9B and C as b are consistent with an equilibrium process with rapid insertion/deinsertion of CO_2 occurring.³² This observation also indirectly supports a monomeric structure for the insertion product (**9**), since a dimer structure would be expected to be more stable toward decarboxylation. The sharp ^{13}C signal for the carbonate and broad

(31) Unlike what we have reported for the analogous cadmium bis(phenoxide) pyridine derivative,¹⁶ no phenoxide complex of zinc possessing a coordination number greater than 4 has been observed.

(32) On the basis of the chemical shift differences in hertz between the inserted and free CO_2 , the rate constant for insertion/deinsertion of CO_2 into complex **7** in pyridine solution is considerably slower than 3300 s^{-1} at ambient temperature.

^{13}C resonance for free $^{13}\text{CO}_2$ can be understood as follows. The line shape of the ^{13}C signal of CO_2 in the complex is independent of the $[\text{CO}_2]$; i.e., the lifetime (τ) of CO_2 in complex **9** equals k_{-1}^{-1} , whereas the line shape of the ^{13}C resonance of free CO_2 depends on $[\text{CO}_2]$, where $\tau = [\text{CO}_2]\{k_{-1}[\mathbf{9}]\}^{-1}$.

Comments and Conclusions

In this paper, we have described the preparation and structural characterization of a series of monomeric zinc bis phenolate derivatives containing sterically encumbering substituents at the 2,6-positions of the ring to inhibit aggregate formation. These bis phenoxide complexes were isolated in the solid state as four-coordinate, highly distorted tetrahedra, where zinc's coordination sphere is completed by two labile donor ligands such as THF. In noninteracting solvents such as benzene or methylene chloride, these ancillary ligands are extensively dissociated from the zinc center, with the degree of ligand dissociation being a function of the substituents on the phenoxide groups. Unexpectedly, stronger ligand binding is exhibited by zinc centers containing electron-donating *tert*-butyl substituents on the phenolate ligands as opposed to electron-withdrawing phenyl substituents.³³ This is a general observation for a wide range of ancillary ligands (from cyclic ethers to tertiary phosphines) for both zinc and cadmium monomeric bis phenoxide derivatives.^{15,22} In all instances, the order of ligand binding is $\text{py} > \text{THF} > \text{epoxides}$, although the difference in ΔG° for binding equilibria between ethers and epoxides is less than 5 kJ/mol.^{16,34,35}

Hence, the solution properties of these monomeric zinc species exhibited in noninteracting media, in particular liquid epoxides and CO_2 , make them good catalysts for ring-opening epoxides in either homopolymerization or copolymerization with carbon dioxide processes to afford polyethers or polycarbonates, respectively. Indeed, as we have demonstrated herein, these zinc derivatives are among the very best catalysts for the copolymerization of cyclohexene oxide and CO_2 for the production of high-molecular-weight polycarbonates with low levels of polyether linkages.³⁶ The order of catalytic activity as a function of the phenolate ligands on zinc was found to be 2,4,6-trimethylphenoxide \gg 2,6-di-*tert*-butylphenoxide $>$ 2,6-diphenylphenoxide $>$ 2,6-di-isopropylphenoxide. This trend in catalytic activity is a balance between an electron-rich metal center, which is more reactive toward both epoxide ring-opening and CO_2 insertion processes, and the steric hindrance about the metal center, which retards both processes. Although we^{2,8,9} have come a long way in developing more active, better defined catalysts for the copolymerization of selected epoxides and CO_2 , a process which affords high-molecular-weight polymers ($M_w > 50\,000$) with low polydispersity ($M_w/M_n < 1.2$) for a variety of epoxides has yet to be uncovered (see Note Added in Proof).

Because of the facility of the back-biting reaction of the intermediate resulting from CO_2 insertion into the zinc-promoted ring-opening of propylene oxide as compared to polymer growth, these zinc derivatives were only effective at producing

(33) Molecular modeling studies indicate that the two-coordinate zinc complexes resulting from ancillary ligand dissociation should be too sterically hindered to afford dimer structures. Furthermore, we have generally found these aggregate structures, when formed from smaller phenoxide ligands, not to be soluble in nonpolar solvents such as benzene.

(34) Denisov, V. M.; Kuznetsov, Yu. P. *Izv. Akad. Nauk. SSSR, Ser. Khim.* **1975**, 25, 2595.

(35) Duman, P.; Guerin, P. *Can. J. Chem.* **1978**, 56, 925.

(36) The only catalyst system which is comparable to the one presented here is the system described in ref 8.

propylene carbonate.³⁷ Nevertheless, these bis phenoxide derivatives of zinc were competent at terpolymerization of cyclohexene oxide/propylene oxide/CO₂, with little cyclic propylene carbonate formation as long as the propylene oxide was maintained at less than 50% mole fraction. Of importance to a system capable of catalyzing the production of poly(propylene carbonate), which in general provides sizable quantities of cyclic propylene carbonate as a byproduct, we have shown this byproduct to be a good ligand toward zinc, and much better than an epoxide. As a consequence, propylene carbonate should be a very effective competitive inhibitor for these copolymerization processes. Similarly, the preferential binding of the zinc center in these bis phenoxide derivatives to donor solvents as compared to epoxides is amply demonstrated by the observation that copolymerization reactions attempted in THF or dioxane were completely unsuccessful.

Pertinent to the initiation step of the copolymerization process, we have confirmed that, in the absence of coordinating solvents, both sterically hindered and unhindered phenoxide derivatives of zinc catalyze the homopolymerization of epoxides to polyethers. That is, homopolymerization of epoxides requires a site on zinc for epoxide binding. Indeed, the *tert*-butyl-substituted phenoxide ligand was found to be the most active of the group investigated herein for homopolymerization of epoxides. On the other hand, CO₂ insertion into the Zn–O(phenoxide) bond does not require a site on zinc for coordination but necessitates

(37) In general, for a large variety of catalyst systems, the yields of copolymer of propylene oxide/CO₂ are much less than 50 g of polymer/g of zinc for conditions similar to those employed here; e.g., see ref 3–7.

accessible lone pairs on the phenoxide's oxygen atom. Therefore, small substituents (e.g., Me) on the 2,6-positions of the phenyl ring allow for CO₂ insertion to provide a metal aryl carbonate intermediate, whereas large substituents (e.g., *tert*-butyl, phenyl) do not. Hence, in the latter instances, initiation has to involve epoxide ring-opening prior to CO₂ insertion. In subsequent steps, where the newly formed metal alkoxide is not sterically congested, CO₂ insertion into the metal–O bond readily occurs. For sure, in the absence of steric inhibition, CO₂ insertion (eq 5) is more facile than epoxide ring-opening (eq 6).

Acknowledgment. Financial support of this research by the National Science Foundation (Grant 96-15866) and the Robert A. Welch Foundation is greatly appreciated.

Note Added in Proof

Subsequent to the submission of this manuscript, a well-defined, very active zinc catalyst was reported for the copolymerization of cyclohexene oxide/CO₂ which provides a copolymer of low polydispersity (Cheng, M.; Lobkovsky, E. B.; Coates, G. W. *J. Am. Chem. Soc.* **1998**, *120*, 11018).

Supporting Information Available: Ball-and-stick drawings and tables of anisotropic thermal parameters, bond lengths, and bond angles for complexes **1–4**, **6**, and **7** (36 pages, print/PDF). See any current masthead page for ordering information and Web access instructions.

JA9826284